THE JOURNAL OF BIOLOGICAL CHEMISTRY VOL. 284, NO. 1, pp. 199–206, January 2, 2009

Reconstitution of Human Ero1-Lα/Protein-Disulfide Isomerase Oxidative Folding Pathway *in Vitro*

POSITION-DEPENDENT DIFFERENCES IN ROLE BETWEEN THE a AND a′ DOMAINS OF PROTEIN-DISULFIDE ISOMERASE[*S]

Received for publication, August 27, 2008, and in revised form, November 4, 2008 Published, JBC Papers in Press, November 11, 2008, DOI 10.1074/jbc.M806645200

Lei Wang[‡§], **Sheng-jian Li**[‡§], **Ateesh Sidhu**[¶], **Li Zhu**[‡§], **Yi Liang**[‖], **Robert B. Freedman**[¶], **and Chih-chen Wang**[‡1]

From the [‡]*National Laboratory of Biomacromolecules, Institute of Biophysics, Chinese Academy of Sciences, Beijing 100101, China, the* [§]*Graduate School of the Chinese Academy of Sciences, Beijing 100049, China, the* [¶]*Department of Biological Sciences, Warwick University, Coventry CV4 7AL, United Kingdom, and the* [‖]*State Key Laboratory of Virology, College of Life Sciences, Wuhan University, Wuhan 430072, China*

Protein-disulfide isomerase (PDI), a critical enzyme responsible for oxidative protein folding in the eukaryotic endoplasmic reticulum, is composed of four thioredoxin domains *a*, *b*, *b′*, *a′*, and a linker *x* between *b′* and *a′*. Ero1-Lα, an oxidase for human PDI (hPDI), has been determined to have one molecular flavin adenine dinucleotide (FAD) as its prosthetic group. Oxygen consumption assays with purified recombinant Ero1-Lα revealed that it utilizes oxygen as a terminal electron acceptor producing one disulfide bond and one molecule of hydrogen peroxide per dioxygen molecule consumed. Exogenous FAD is not required for recombinant Ero1-Lα activity. By monitoring the reactivation of denatured and reduced RNase A, we reconstituted the Ero1-Lα/hPDI oxidative folding system *in vitro* and determined the enzymatic activities of hPDI in this system. Mutagenesis studies suggested that the *a′* domain of hPDI is much more active than the *a* domain in Ero1-Lα-mediated oxidative folding. A domain swapping study revealed that one catalytic thioredoxin domain to the C-terminal of *bb′x*, whether *a* or *a′*, is essential in Ero1-Lα-mediated oxidative folding. These data, combined with a pull-down assay and isothermal titration calorimetry measurements, enabled the minimal element for binding with Ero1-Lα to be mapped to the *b′xa′* fragment of hPDI.

Disulfide bonds play an essential role in the folding and assembly of secretory proteins and membrane proteins. The formation of non-natural disulfide bonds leads to protein misfolding and further aggregation. Both prokaryotes and eukaryotes possess specialized cellular compartments in which disulfide bonds are formed, complete with enzymes devoted to catalyzing disulfide formation and rearrangement (1).

In eukaryotes, oxidative protein folding occurs in the endoplasmic reticulum (ER),[2] facilitated by protein-disulfide isomerase (PDI, EC 5.3.4.1) and/or its homologues, ERp57, PDIp, ERp72, PDIr, P5, ERp44, etc. (2, 3). PDI comprises four thioredoxin (Trx) domains, two catalytic domains, *a* (9–116) and *a′* (352–462), separated by two homologous non-catalytic domains, *b* (120–217) and *b′* (219–332), plus a C-terminal region (463–491). In addition, there is a short linker region "*x*" (333–351) between the *b′* and *a′* domains (4, 5). As an abundant multifunctional protein within the lumen of the ER, PDI acts as both an enzyme and a chaperone in many physiological processes (6–8). PDI can act *in vitro* to catalyze both protein-disulfide isomerization and net protein disulfide formation, but the latter process requires a further source of oxidizing equivalents to reoxidize PDI. Hence a net source of oxidizing equivalents is required *in vivo* to sustain formation of protein disulfides and oxidative protein folding. Ero1p was found to be directly responsible for the production of disulfide bonds in the *Saccharomyces cerevisiae* ER (9, 10). The catalytic cycle carried out by Ero1p involves direct oxidation of PDI by the shuttle cysteine pair (Cys^{100}-Cys^{105}), and re-oxidation of the reduced shuttle cysteine residues through internal dithiol-disulfide exchange with the active site (Cys^{352}-Cys^{355}). The latter are re-oxidized by transfer of their electrons to the flavin adenine dinucleotide (FAD) cofactor and further to molecular oxygen, resulting in the formation of hydrogen peroxide. Ero1p activity can be modulated through the redox state of two non-essential "regulatory" cysteine pairs (Cys^{90}-Cys^{349} and Cys^{150}-Cys^{295}) by controlling the range of motion for the shuttle-cysteine-containing loop region (11).

In mammalian cells, there are two homologues of Ero1p, Ero1-Lα, and Ero1-Lβ, which show different tissue distribution and transcriptional regulation (12, 13). Both Ero1-Lα and Ero1-Lβ accelerate oxidative protein folding in the ER of human cells through their action on PDI (14). Although it was

* This work was supported by Grants 2006CB910903, 2006CB806508, and 2006CB910301 from the Chinese Ministry of Science and Technology; 30620130109 from the Chinese Natural Science Foundation; BB/D017807/1 from the UK BBSRC (Biotechnology and Biological Sciences Research Council); and by a UK/China Partnering Award (PA1339) from the BBSRC (to A. S., L. W., and R. B. F.). The costs of publication of this article were defrayed in part by the payment of page charges. This article must therefore be hereby marked "*advertisement*" in accordance with 18 U.S.C. Section 1734 solely to indicate this fact.

[S] The on-line version of this article (available at http://www.jbc.org) contains supplemental Figs. S1 and S2.

[1] To whom correspondence should be addressed. Tel.: 86-10-64888502; Fax: 86-10-64840672; E-mail: chihwang@sun5.ibp.ac.cn.

[2] The abbreviations used are: ER, endoplasmic reticulum; PDI, protein-disulfide isomerase; Trx, thioredoxin; hPDI, human PDI; DShPDI, domain-swapped hPDI; GST, glutathione *S*-transferase; DTT, dithiothreitol; AMS, 4-acetamido-4′-maleimidylstilbene-2,2′ disulfonic acid; ITC, isothermal titration calorimetry; yPDI, yeast PDI; PBS, phosphate-buffered saline.

suggested, by analogy to the case in Ero1p, that the two conserved cysteine triads (Cys^{85}-Cys^{94}-Cys^{99} and Cys^{391}-Cys^{394}-Cys^{397}) in Ero1-Lα molecule may cooperate in electron transfer (15), little is known about the biochemistry of human Ero1 proteins in catalyzing oxidative folding and the interaction with human PDI (hPDI). Indeed, very little work has been reported on the reconstitution of this process *in vitro*.

In this work, we report that Ero1-Lα utilizes oxygen as a terminal electron acceptor, producing one disulfide bond and one molecule of hydrogen peroxide using the prosthetic group FAD as an electron transfer component. Furthermore, we have reconstituted the *in vitro* Ero1-Lα/hPDI oxidative folding system, and demonstrated by mutagenesis studies on hPDI and domain-swapped hPDI (DShPDI) that the *a* and *a′* domains of hPDI have distinct activities in Ero1-Lα-mediated oxidative folding and that this is primarily due to their positions in the PDI molecule. Calorimetry and pull-down determinations revealed that the *b′xa′* region is the minimal fragment of hPDI that is able to bind with Ero1-Lα. Our studies provide insights into the interaction of these two important catalysts of the mammalian oxidative protein folding machine.

EXPERIMENTAL PROCEDURES

Protein Expression and Purification—The cDNA encoding the Ero1-Lα sequence 24–468 without the signal sequence from pcDNA3.1ERO1-Lα-Myc (a kind gift from Prof. R. Sitia, Università Vita-Salute San Raffaele, Minalo, Italy) was inserted into pGEX-6P-1 vector (Amersham Biosciences) at BamHI and XhoI sites. The glutathione *S*-transferase (GST)-Ero1-Lα fusion construct was expressed in BL21 (DE3) pLysS (Novagen). Cultures were grown in 2 liters of 2× YT medium at 37 °C for 4 h and shaken for an additional 20 h at 25 °C after isopropyl-β-D- thiogalactoside was added to a final concentration of 40 μM. The supernatant of the cell lysate was applied onto a glutathione-Sepharose 4 Fast Flow column (Amersham Biosciences) pre-equilibrated with phosphate-buffered saline solution (PBS, 140 mM NaCl, 2.7 mM KCl, 10 mM Na_2HPO_4, 1.8 mM KH_2PO_4, pH 7.3). After washing with 5–10 column volumes of PBS, the GST-Ero1-Lα fusion protein was eluted with 50 mM Tris-HCl, 10 mM GSH, pH 8.0. The elution was dialyzed against buffer A (50 mM Tris-HCl and 150 mM NaCl, pH7.6) to remove GSH, and then digested with 100 μl (200 units) of PreScission Protease (Amersham Pharmacia Biosciences) at 4 °C for 4 h followed by chromatography on a glutathione 4 Fast Flow column pre-equilibrated with buffer A to remove the GST moiety and the PreScission Protease. The flow-through was concentrated and stored as aliquots in buffer A at −80 °C. The final purified Ero1-Lα protein has an additional GPLGS pentapeptide at the N terminus after removing the GST tag.

Recombinant full-length hPDI was purified as described (16). hPDI-*bb′x*, hPDI-*a* and hPDI-*a′c* proteins were expressed from clones kindly provided by Prof. L. W. Ruddock (University of Oulu, Finland). The appropriate coding regions were inserted into pLWR51p (a modified version of pET23b (Novagen)), and the proteins were expressed and purified as described previously (5); the resulting proteins all included an N-terminal His tag (MHHHHHHM). All other hPDI and DShPDI mutants were constructed by overlap extension PCR using pQE30-hPDI plasmid as a template and subsequently inserted into pQE30 vector (Qiagen). The mutated proteins, containing an N-terminal His tag (MRGSHHHHHHGS), were expressed and purified using the same protocol as for the full-length hPDI.

The sequences of all the constructs were verified by DNA sequencing. Protein concentrations were determined by the Bradford method with bovine serum albumin as a standard (17).

Oxygen Consumption Assay—Escherichia coli Trx (a kind gift from Dr. Xi Wang in this group) was reduced by DTT as described (18). Oxygen consumption was measured by using an Oxygraph Clark-type oxygen electrode (Hansatech Instruments). All components of each reaction, except Ero1-Lα, were fresh mixed in a total volume of 0.5 ml, and the reaction was initiated by injection of Ero1-Lα into the reaction vessel of the oxygen electrode. For detection of hydrogen peroxide, 5 μl of catalase at 2 mg/ml was injected into the reaction vessel at 10 min, when the thiol oxidation reaction was complete. All experiments were performed in buffer B (100 mM Tris-HAc, 50 mM NaCl, and 1 mM EDTA, pH 8.0).

RNase A Assay—Denatured and reduced RNase A was prepared as described (19). RNase A reactivation was assayed quantitatively by monitoring the absorbance increase at 296 nm at 25 °C due to the hydrolysis of cCMP, and the isomerase and oxidoreductase activities of hPDI proteins are calculated as previously reported (20). The relative activity (%) was calculated as (A-A0)/(A1-A0) × 100%, where A, activity of hPDI mutants or DShPDI mutants; A1, activity of hPDI or DShPDI; A0, activity of hPDIC1/2 or DShPDIC1/2, respectively. Data are expressed as mean ± S.D. ($n = 3$).

Gel-based RNase A re-oxidation analyses were performed by addition of Ero1-Lα, hPDI, and/or FAD into buffer B containing 15 μM denatured and reduced RNase A. At the indicated time points, free thiols were blocked by the addition of 6× SDS-loading buffer containing 12 mM 4-acetamido-4′-maleimidylstilbene-2,2′ disulfonic acid (AMS, invitrogen). The oxidized and reduced forms of RNase A were detected by Coomassie Blue staining after non-reducing SDS-PAGE.

GST-Pull-down Assay—GST-Ero1-Lα fusion protein on glutathione-Sepharose resin was incubated with hPDI proteins for 2 h at 4 °C in PBS, washed with PBS for three times, and bound proteins were detected by Coomassie Blue staining after reducing SDS-PAGE.

Isothermal Titration Calorimetry (ITC) Measurement—Thermodynamic parameters associated with the reactions between hPDI proteins and Ero1-Lα were measured on a VP-ITC titration calorimeter (MicroCal, Inc.) at 25 °C. A solution of 12 μM Ero1-Lα was loaded into the sample cell (1.43 ml), and a solution of 75–120 μM hPDI proteins was placed in the injection syringe (295.7 μl). The first injection (5 μl) was followed by 29 injections of 10 μl. Dilution heats of the hPDI proteins were measured by injecting the hPDI proteins into buffer alone and were subtracted from the experimental curves prior to data analysis. Data were analyzed using MicroCal ORIGIN software supplied with the instrument. All experiments were performed in buffer A. The stirring rate was 300 rpm.

RESULTS

Characterization of Ero1-Lα—After cleavage of the GST tag, the Ero1-Lα protein was bright yellow; it exhibited a single band of about 55 kDa on reducing SDS-PAGE (supplemental Fig. S1) and two peaks, corresponding to apparent molecular mass of 44 kDa and 100 kDa, respectively, on a Superdex 75 HR 10/30 column, indicating that the preparation is largely composed of monomer with less than 20% dimer (Fig. 1*A*). Because the content of dimer decreased but did not disappear after DTT treatment, the dimer is mainly a disulfide-linked homodimer with a small fraction of non-covalent homodimer (also see supplemental Fig. S1).

As shown in Fig. 1*B*, the absorption of Ero1-Lα preparation exhibits a typical unresolved flavin spectrum with the maximum absorbance at 454 nm with a shoulder at 485 nm and another peak at ~370 nm, in addition to the protein peak at 280 nm. Each Ero1-Lα molecule contains 0.9 FAD determined by using the extinction coefficient of 12.5 mM^{-1} cm^{-1} at 454 nm (18). Dialysis of Ero1-Lα against 2 mM EDTA buffer revealed that FAD binds tenaciously to the enzyme. After treatment by 6 M guanidine hydrochloride, the spectrum became like that of free FAD indicated by the shift of the maximum absorbance from 454 nm to ~447 nm and disappearance of the shoulder at 485 nm.

As shown in Fig. 1*C* the absorbance at 454 nm of 10 μM Ero1-Lα started decreasing after 4 min of 2 mM DTT treatment, suggesting the reduction of bound FAD to $FADH_2$. The lag corresponds to the time required to remove solution-dissolved oxygen. In contrast, no absorbance change was detected for 10 μM free FAD over the course of the experiment. The results indicated that electrons can be transferred from reducing agent to Ero1-Lα-bound FAD but not to free FAD. Thus, Ero1-Lα contains an equimolar FAD as its prosthetic group, and the bound FAD is redox active.

Oxygen Is Reduced to Form Hydrogen Peroxide during Ero1-Lα-catalyzed Thiol Oxidation—There were conflicting reports on whether hydrogen peroxide was a byproduct of the thiol oxidation driven by yeast Ero1p (18, 21). We monitored the oxygen consumption of a system containing Ero1-Lα and thiol reagents. As shown in Fig. 2*A*, a drop of 49 μM oxygen (after subtracting the background oxygen consumption by a nonenzymatic reaction) was detected during Ero1-Lα-catalyzed oxidation of 50 μM reduced *E. coli* Trx (Trx_{red}), and addition of catalase at 10 min restored 20 μM oxygen in the solution, indicating a production of 40 μM hydrogen peroxide ($2H_2O_2 \rightarrow 2H_2O + O_2$). Thus, the general reaction ($2R\text{-}SH + O_2 \rightarrow R\text{-}S\text{-}S\text{-}R + H_2O_2$) catalyzed by flavoprotein sulfhydryl oxidases applies also to Ero1-Lα.

Table 1 compares the catalytic activities of our recombinant Ero1-Lα with recombinant Ero1p. GSH is a rather poor substrate of Ero1-Lα, similar to Ero1p (22), while DTT and Trx_{red} are good substrates of Ero1-Lα. The K_m for oxygen was determined by observing the rate of reaction as oxygen was depleted from the system (Fig. 2*B*). The low K_m of 5 μM for oxygen is similar to that of Ero1p (Table 1), suggesting that Ero1-Lα can function efficiently at low oxygen tension, minimizing the risk

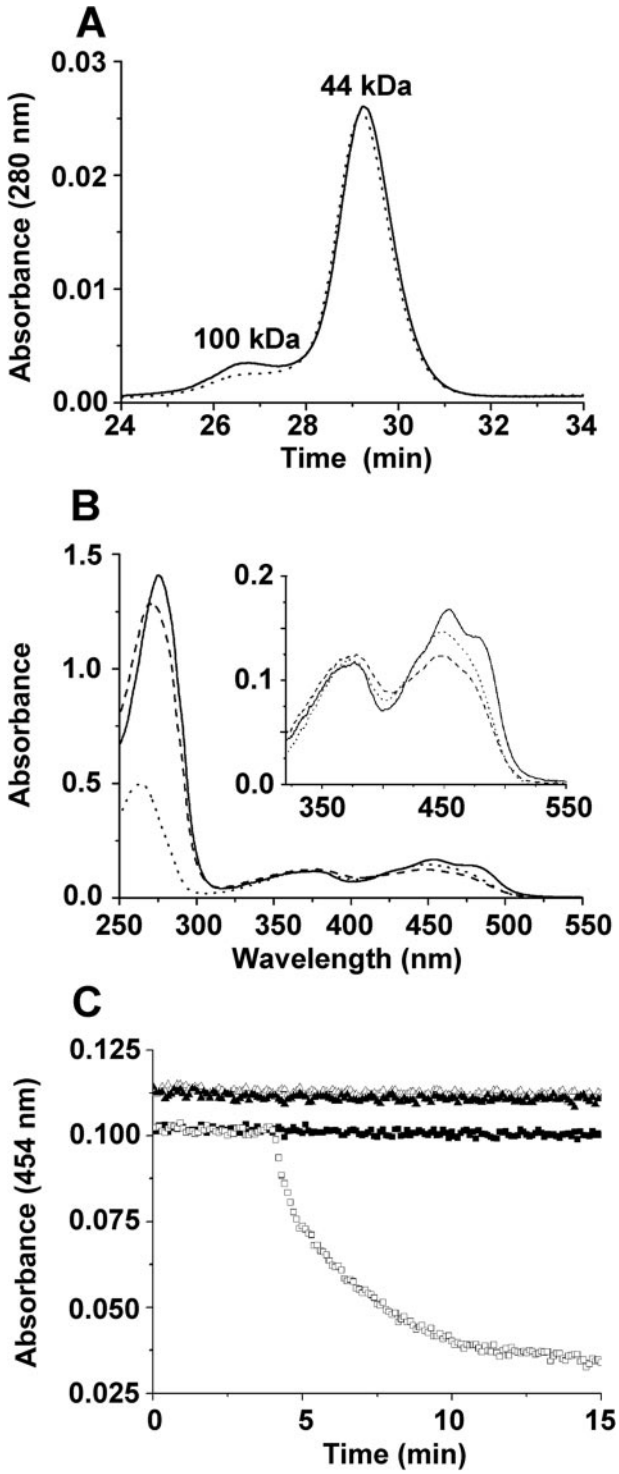

FIGURE 1. **Biochemical characterization of the Ero1-Lα preperation.** *A*, size-exclusion chromatography of Ero1-Lα was performed in the absence (— —) or presence (····) of 10 mM DTT on a Superdex 75 HR 10/30 column at room temperature using Tris-HCl buffer containing 0.2 M NaCl at 0.5 ml/min. Molecular weight markers (Amersham Biosciences) were albumin, 67 kDa; ovalbumin, 43 kDa; chymotrypsinogen A, 25 kDa, and RNase A, 13.7 kDa. *B*, absorbance spectrum of Ero1-Lα at 15.4 μM was measured in the absence (— —) or presence (····) of 6 M guanidine hydrochloride, with the spectrum of 12.9 μM free FAD (●) (11.3 mM^{-1} cm^{-1} for extinction coefficient at 446 nm) as a control. The spectrum in the visible region is enlarged in the *inset*. *C*, reduction of Ero1-Lα-bound FAD by DTT. Absorbance changes at 454 nm of Ero1-Lα (*squares*) and free FAD (*triangles*) at 10 μM in buffer A were monitored in the absence (*filled*) or presence (*open*) of 2 mM DTT, respectively.

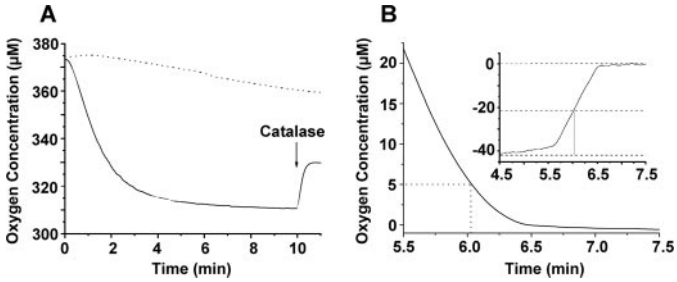

FIGURE 2. **Oxygen is reduced by Ero1-Lα to form hydrogen peroxide.** *A*, oxygen consumption was monitored immediately after injection of 1 μM Ero1-Lα into buffer B with (——) or without (····) 50 μM Trx_{red}. Catalase was added at the indicated time (*arrow*). *B*, K_m determination for oxygen. Ero1-Lα at 1 μM was injected into buffer B containing 10 mM DTT. The graph shows the end of the reaction, when the oxygen has been depleted to <10% of its initial value. The *inset* is the first derivative of the data, used to identify the point, at which the rate was half-maximal.

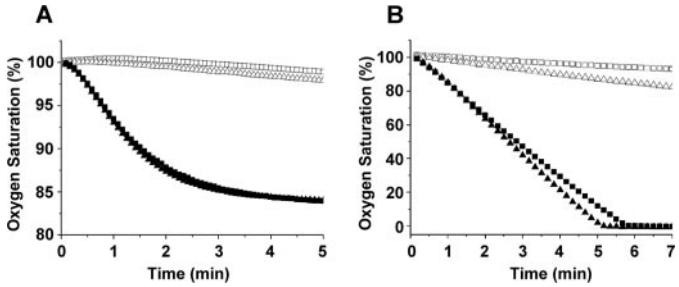

FIGURE 3. **Effect of exogenous FAD on the rate of oxygen consumption in Ero1-Lα-catalyzed disulfide formation.** Oxygen consumption was monitored immediately after injection of Ero1-Lα (*filled symbols*) to a final concentration of 1 μM into 50 μM Trx_{red} (*A*) or 10 mM DTT (*B*), in the absence (*squares*) or presence (*triangles*) of 100 μM FAD. Traces measured in the absence of Ero1-Lα are indicated by *open symbols*.

TABLE 1
Comparison of substrate kinetics of Ero1-Lα and Ero1p

	Ero1-Lα			Ero1p		
	k_{cat}[a]	K_m	k_{cat}/K_m	k_{cat}	K_m	k_{cat}/K_m
	min^{-1}	μM	$M^{-1}min^{-1}$	min^{-1}	μM	$M^{-1}min^{-1}$
DTT (10 mM)	41	5	8×10^6	17[b,c]	4[b,c]	4×10^6 [b,c]
Trx_{red} (50 μM)	37	-	-	12[b]	-	-
GSH (10 mM)	1	-	-	-	-	-

[a] k_{cat} are expressed in terms of oxygen molecules consumed per min. The K_m values are for oxygen.
[b] Taken and calculated based on the data from Gross *et al.* (18).
[c] 12.5 mM DTT.
–, not determined.

of reductive stress in the ER. Moreover, the turnover number of Ero1-Lα for oxygen is about 3-fold that of Ero1p.

Effect of Exogenous FAD on the Reaction Catalyzed by Ero1-Lα—Ero1p purified from yeast has been reported to be active only in the presence of exogenous FAD (21, 22), however, two C-terminal-truncated Ero1p mutants expressed in *E. coli* showed activity without addition of FAD (18). We tested the effect of exogenous FAD on the activity of recombinant Ero1-Lα using oxygen consumption assay. As shown in Fig. 3, the presence of 100 μM exogenous FAD did not affect the oxygen consumption rate in Ero1-Lα-catalyzed oxidation of either 50 μM Trx_{red} or 10 mM DTT. Also, exogenous FAD was not required for the reactivation of RNase A driven by Ero1-Lα (see below). Hence the FAD found bound to recombinant Ero1-Lα is fully functional.

Reconstitution of the Ero1-Lα/hPDI Oxidative Folding Pathway in Vitro—By monitoring the reactivation of denatured and reduced RNase A, which requires the formation of four specific disulfides necessary for its activity, we reconstituted the Ero1-Lα/hPDI system *in vitro*, and attempted to resolve the isomerase and oxidoreductase activities of hPDI in this system. As shown in Fig. 4*A*, either Ero1-Lα or hPDI alone did not promote reactivation of RNase A. The presence of Ero1-Lα and hPDI together did catalyze reactivation of RNase A, and the reactivation rate increased with increasing concentrations of Ero1-Lα. Exogenous FAD is not required for the reactivation of RNase A in this system. The direct observation of distribution of reduced and oxidized RNase A during reactivation (Fig. 4*B*) supported the above results. The data show that the reactivation of RNase A results from the oxidative formation of disulfide bonds, which requires both hPDI as catalyst and either Ero1-Lα or a glutathione buffer to deliver oxidizing equivalents. The transfer of oxidizing equivalents in the system of Ero1-Lα/hPDI is similar to what has been observed in the case of Ero1p (22). We then isolated the monomer Ero1-Lα fraction by gel filtration and subsequently assayed this monomer fraction in the reconstituted system. The monomer Ero1-Lα is somewhat more active than the unfractionated preparation (supplemental Fig. S2), indicating that the monomer fraction contributes the dominating activities in our Ero1-Lα preparation and the dimer fraction is either inactive or less active than the monomer fraction. However, this does not exclude the possibility that Ero1-Lα homodimer could have a potential function *in vivo*, which needs further investigation and is beyond the scope of this research.

The experiments shown in Fig. 4*A* represent a one-pot assay in which reduced RNase A is oxidized and re-activated, and the active RNase A then hydrolyzes its substrate, giving rise to a change in absorbance; the data shown represent the instantaneous RNase A activity as a function of time (19, 23). The data show a lag phase followed by a period in which RNase A activity increases linearly. The lag is interpreted as a period during which reduced RNase A is oxidized to produce a mix of inactive disulfide isomers, while the linear phase represents isomerization of these species to native active RNase A. We have calculated the rate of RNase A reactivation (essentially the isomerase activity of hPDI) by measuring the rate of increase of RNase A activity during the linear phase, and the rate of RNase A oxidation (the oxidoreductase activity of the complete system) by measuring the reciprocal of the lag time before the appearance of active RNase A. As shown in Fig. 4*C*, increasing concentrations of Ero1-Lα significantly enhanced the oxidoreductase activity, but did not significantly influence the isomerase activity of hPDI. The isomerase and oxidoreductase activities of hPDI in the presence of the optimal glutathione redox buffer (1 mM GSH/0.2 mM GSSG) are shown in Fig. 4*C* for comparison, and it is apparent that the isomerase activity is approximately invariant and is basically independent of the nature of the source of oxidizing equivalents.

Ero1-Lα-mediated and hPDI-catalyzed Oxidative Folding Is Strongly Influenced by the Positions of Catalytic Trx Domains in hPDI—To explore the structural and functional requirements for the interaction of hPDI with Ero1-Lα, we examined the

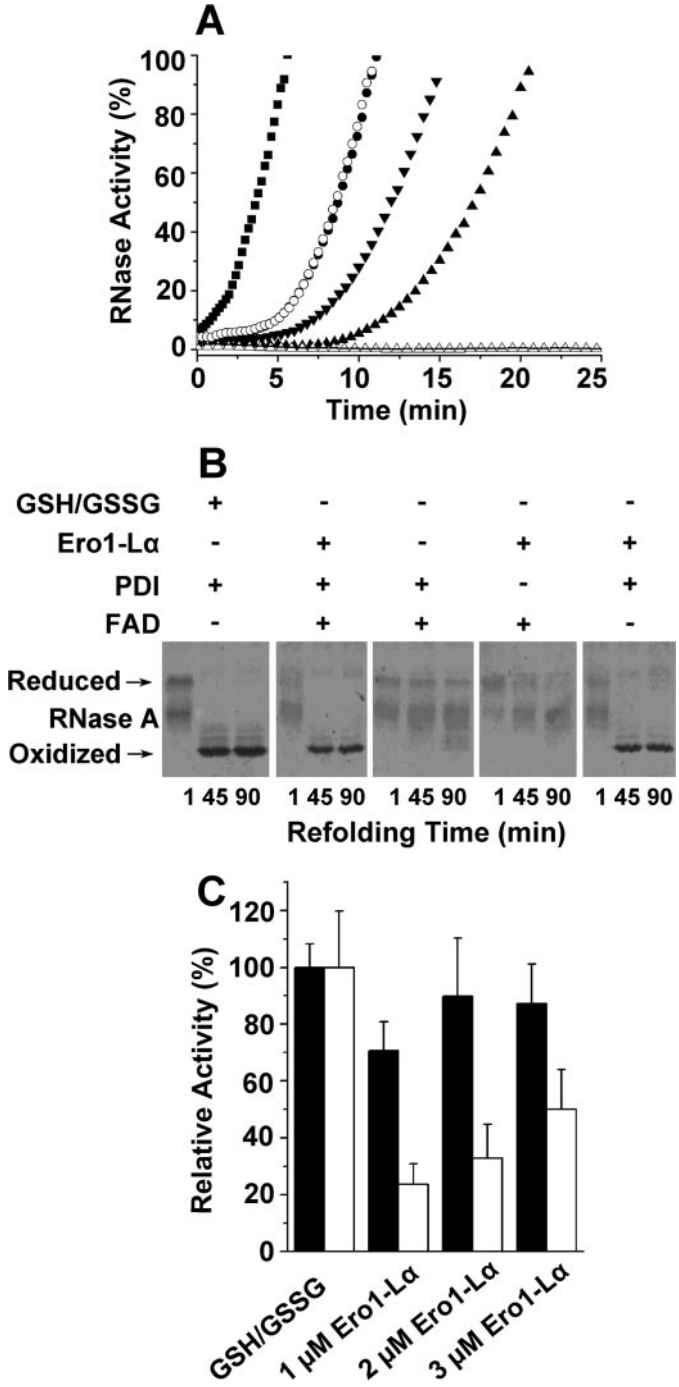

FIGURE 4. **Reconstitution of oxidative protein folding system *in vitro*.** *A*, reactivation of denatured and reduced RNase A (8 μM) in buffer B was determined by monitoring the hydrolysis of cCMP (4.5 mM) in the presence of hPDI (3 μM) and FAD (100 μM) (△); Ero1-Lα (3 μM) and FAD (100 μM) (–); hPDI (3 μM), FAD (100 μM), and Ero1-Lα at 1 μM (▲), 2 μM (▼), or 3 μM (●); hPDI (3 μM) and Ero1-Lα (3 μM) (○), respectively. RNase A refolding in the presence of hPDI (3 μM) and an optimal glutathione redox buffer (1 mM GSH/0.2 mM GSSG) (■) was for comparison. The data points plotted are the instantaneous RNase activities derived as the derivative of the plot of absorbance *versus* time. *B*, refolding of RNase A (15 μM) was carried out in the absence or presence of Ero1-Lα (3 μM), hPDI (3 μM), and/or FAD (100 μM) as indicated, quenched at different times with AMS, and analyzed by 15% non-reducing SDS-PAGE. *C*, comparison of the isomerase (*filled*) and oxidoreductase (*open*) activities of hPDI in the presence of different concentrations of Ero1-Lα. The enzyme activities in the presence of an optimal glutathione redox buffer were taken as 100%.

reactivation of RNase A in the reconstituted system containing Ero1-Lα and different hPDI domain combinations and mutants (Fig. 5, *upper panel*). The activities of the various PDI constructs were studied in the presence either of the glutathione redox buffer or of Ero1-Lα. In the optimal glutathione redox buffer, hPDI-ΔC showed similar activities to those of the full-length hPDI. Those constructs that contain only one intact dithiol active site (hPDI-*bb′xa′* and hPDI-*abb′x*) or one intact site plus one -CGHC- mutated to -SGHS- (hPDIC1 and hPDIC2), all showed similar abilities to catalyze the reactivation of RNase A. Hence, all combinations of one active Trx domain plus the core *bb′x* region showed roughly equivalent isomerase and oxidoreductase activities in GSH/GSSG-driven oxidative protein folding. The single domains (hPDI-*a* and hPDI-*a′c*) showed low oxidoreductase activity (<20%) and very low isomerase activity (<5%). The mutant full-length PDI with two active sites both mutated to -SGHS- (hPDIC1/2) showed no activity at all and was taken as a negative control.

In the system in which Ero1-Lα supplied the oxidative equivalents, hPDI-ΔC did not show any inferiority to the full-length hPDI, indicating that the C-terminal tail is not involved in the interaction with Ero1-Lα. However, in this system, the various constructs containing a single redox-active Trx domain were not equivalent in activity, in contrast to the situation with the glutathione system as oxidant. Absence of domain *a′* (hPDI-*abb′x*) or mutation of the active site in domain *a′* (hPDIC2) decreased the activity markedly (to <10% of wild-type). Conversely, hPDI-*bb′xa′* and hPDIC1 with the active site in domain *a′* intact are both ~50% active as wild-type, suggesting that the *a′* domain is responsible for the dominating flow of electrons to Ero1-Lα. Moreover, the single domains (hPDI-*a* and hPDI-*a′c*) did not show any detectable activity in this system.

The difference between domains *a* and *a′* of hPDI in Ero1-Lα-mediated oxidative folding is not likely a result of their distinct abilities to interact with the RNase A substrate or facilitate RNase A reactivation, since they behave similarly in the optimal glutathione redox buffer (Fig. 5, *upper panel*). Thus, it is reasonable to hypothesize that the difference arises from their interaction with Ero1-Lα and may depend either on some intrinsic difference between the domains or on their position, *i.e.* whether the active Trx domain is located N-terminal or C-terminal of the *bb′x* fragment. To distinguish between these factors, we produced a series of DShPDI combinations and mutants (Fig. 5, *lower panel*), with the *a* and *a′* domains exchanged positionally. Because DShPDI showed defective activity compared with hPDI we then took the activity of DShPDI as 100% for evaluating the activities of all DShPDI proteins. In the optimal glutathione redox buffer, compared with DShPDIC1/2 with both active sites mutated, DShPDI-*bb′xa* and DShPDI-*a′bb′x* were both able to promote RNase A reactivation, and the former is about 3-fold more active than the latter. Similar to the case in un-swapped proteins, addition of an inactive *a′* or *a* domain in the "swapped position" to one of these constructs (DShPDIC1 and DShPDIC2) does not enhance nor reduce activity further. In Ero1-Lα-mediated oxidative folding, DShPDI-*bb′xa* is over 10-fold more active than DShPDI-*a′bb′x*, and again the addition of the missing domain in mutated form has little effect. All the above results strongly

	1 mM GSH/0.2 mM GSSG		3 μM Ero1-Lα	
	Rate of RNase Reactivation (%)	Rate of RNase Oxidation (%)	Rate of RNase Reactivation (%)	Rate of RNase Oxidation (%)
hPDI	100	100	100	100
hPDI-ΔC	106 ± 26	140 ± 18	94 ± 12	188 ± 38
hPDI-*bb'xa'*	46 ± 15	34 ± 12	34 ± 9	62 ± 23
hPDI-*b'xa'*	41 ± 5	51 ± 3	50 ± 10	39 ± 5
hPDI-*abb'x*	20 ± 2	42 ± 11	2 ± 1	5 ± 3
hPDIC1	51 ± 12	27 ± 8	43 ± 6	22 ± 3
hPDIC2	36 ± 14	29 ± 11	1 ± 1	8 ± 5
hPDIC1/2	0	0	0	0
hPDI-*a*	4 ± 1	18 ± 5	0	0
hPDI-*a'c*	4 ± 1	15 ± 5	0	0
DShPDI	100	100	100	100
DShPDI-*bb'xa*	83 ± 16	67 ± 15	121 ± 31	92 ± 21
DShPDI-*a'bb'x*	33 ± 9	21 ± 7	6 ± 2	6 ± 1
DShPDIC1	77 ± 24	58 ± 20	88 ± 22	91 ± 25
DShPDIC2	27 ± 12	21 ± 6	6 ± 4	10 ± 3
DShPDIC1/2	0	0	0	0

FIGURE 5. **Comparison of the enzymatic activities of the hPDI and DShPDI proteins.** Schematic representation of the hPDI and DShPDI proteins is shown on the *left*, the -CGHC- active sites (★) and the mutated -SGHS- sites (☆) are indicated, and corresponding relative enzymatic activities in the presence of an optimal glutathione redox buffer or 3 μM Ero1-Lα are shown on the *right*. Data are expressed as mean ± S.D. ($n = 3$).

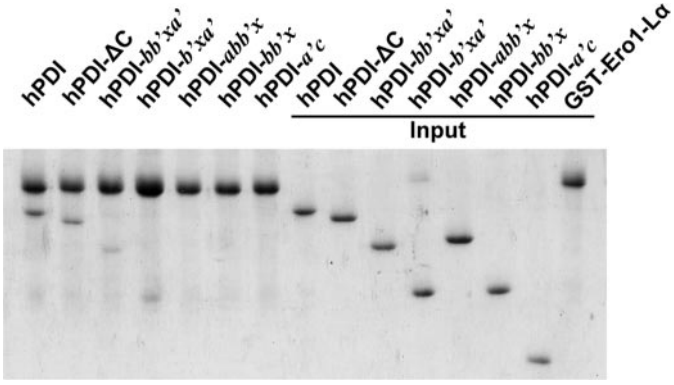

FIGURE 6. **GST-pull-down assay of hPDI proteins binding to Ero1-Lα.** GST-Ero1-Lα fusion protein was incubated with glutathione-Sepharose resin in the absence (the first lane from the *right*) or presence of hPDI proteins as indicated and analyzed by 15% reducing SDS-PAGE. *Input* of hPDI proteins is as indicated.

suggest that either domain *a* or *a'* is able to donate electrons to Ero1-Lα, provided that it is in the position to the C-terminal of the *bb'x* fragment of hPDI, but operates much less efficiently if in the position to the N-terminal of *bb'x*.

b'xa' of hPDI Is the Minimal Element for Binding with Ero1-Lα—We have further investigated the direct interaction of hPDI proteins and Ero1-Lα by GST-pull-down assay. As shown in Fig. 6, full-length hPDI and hPDI-ΔC strongly interacted with Ero1-Lα, whereas hPDI-*bb'xa'* and hPDI-*b'xa'* bound to Ero1-Lα to a lesser extent, and other mutants did not show interaction with Ero1-Lα, consistent with the result obtained by RNase A refolding assay (Fig. 5). The above results indicated that *b'xa'* is the minimal element for efficient interaction with Ero1-Lα. In addition, hPDI-*b'xa'* showed similar enzymatic activities to hPDI-*bb'xa'* in the Ero1-Lα-mediated oxidative refolding of RNase A (Fig. 5).

ITC was then used to describe quantitatively the interaction between Ero1-Lα and hPDI (Fig. 7). The binding of hPDI with Ero1-Lα is an exothermic reaction (Fig. 7*A*), showing favorable van der Waals, hydrogen bond, and electrostatic interactions (24). For the titration of wild-type hPDI and hPDI-ΔC into Ero1-Lα, the integrated binding isotherm was best fit to a four sequential binding sites model, giving a dissociation constant for the first binding event of 0.4 and 1.1 μM, respectively (Fig. 7*B*). The affinity of hPDI-*bb'xa'* and hPDI-*b'xa'* to Ero1-Lα were significantly lower than those of full-length hPDI and hPDI-ΔC, with a dissociation constant for the first binding event 11.1 and 9.7 μM (Fig. 7*B*) derived from a three sequential binding sites model. Because the following binding events may reflect the weak, nonspecific interactions, corresponding to a multisite low affinity binding of substrates to PDI (25), we just presented here the first binding parameters for comparision. No binding reaction for hPDI-*abb'x*, hPDI-*bb'x*, or hPDI-*a'c* with Ero1-Lα was detected by ITC. The affinity of hPDI/Ero1-Lα binding from our data is higher than the binding between ERp57 and the P-domain of calnexin (24) or calreticulin (26), also measured by ITC, suggesting a substantial strong interaction between hPDI and Ero1-Lα.

All the above results strongly supported the idea that the region *b'xa'* of hPDI is the minimal element for binding with Ero1-Lα, and all domains together fulfill the maximum binding.

DISCUSSION

In this study, we have shown that the recombinant Ero1-Lα contains equimolar tightly bound FAD, which is non-covalent but released only on denaturation. Different from Ero1p purified from yeast (21, 22) but similar to recombinant Ero1p purified from *E. coli* (18), the bound FAD in recombinant Ero1-Lα is functionally active, because addition of free FAD does not enhance its activity. Our Ero1-Lα preparation resembles yeast Ero1p in substrate kinetic properties (Table 1) and in the generation of stoichiometric hydrogen peroxide in the presence of dithiol substrates and oxygen.

We have reconstituted an *in vitro* oxidative folding pathway with purified recombinant Ero1-Lα and hPDI, that to our knowledge is the first reconstitution of the folding pathway using mammalian proteins. By using quantitative calculations we have distinguished the isomerization and oxidoreduction processes. The rate of isomerization is independent of the source of oxidizing equivalents, whereas the rate of oxidoreduction is sensitive to the source of oxidation and enhanced with the increase of the concentration of Ero1-Lα. We have shown an asymmetry of the two active sites of hPDI in

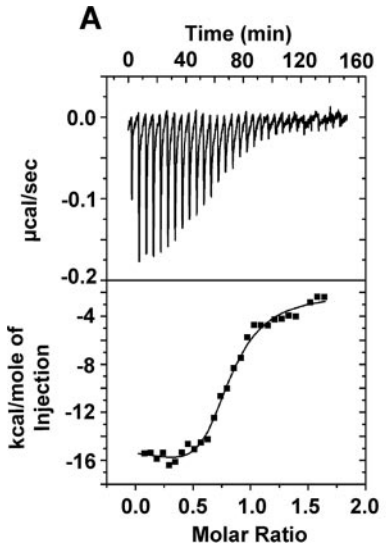

B

hPDIs	*n*	*K*d (μM)	*ΔH* (kcal/mol)
hPDI*	1	0.4 ± 0.1	-16.0 ± 0.4
	(0.95±0.03)	(1.1 ± 0.3)	(-18.6 ± 0.9)
hPDI-ΔC*	1	1.1 ± 0.4	-11.9 ± 2.3
hPDI-*bb'xa'***	1	11.1 ± 8.9	-59.7 ± 23.8
hPDI-*b'xa'***	1	9.7 ± 5.1	-5.0 ± 4.0
hPDI-*abb'x*		NB	
hPDI-*bb'x*		NB	
hPDI-*a'c*		NB	

FIGURE 7. **ITC data of the hPDI proteins binding to Ero1-Lα.** *A*, *upper panel*, heat released per second during the addition of 90 μM full-length hPDI into the ITC cell containing 12 μM Ero1-Lα. *Lower panel*, *squares* represent the integrated binding isotherm at each injection after correction for dilution heat effects and normalization for the molar concentration. *Solid lines* represent the non-linear least squares fit to a four sequential binding sites model. *B*, ITC thermodynamic parameters of hPDI proteins binding to Ero1-Lα. *, data are for the first binding event with fitting to a four sequential binding sites model. The data in *parentheses* are based on a single site model. **, data are for the first binding event with fitting to a three sequential binding sites model. *NB*, no binding observed.

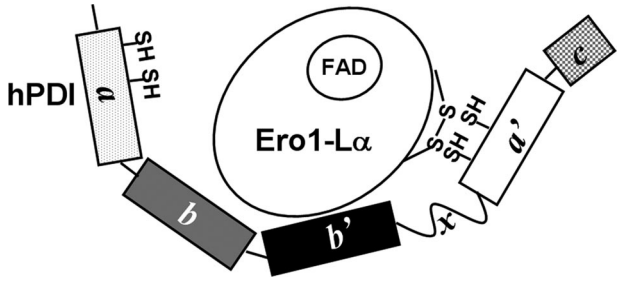

FIGURE 8. **Schematic model illustrating the interaction between Ero1-Lα and hPDI.** The four Trx domains of hPDI are arranged in a "U" shape, with the two active sites in *a* and *a'* domains facing each other, according to the crystal structure of yPDI (PDB code: 2B5E) and molecular modeling (SWISS-MODEL) (data not shown). The *b'xa'* fragment of hPDI provides the essential binding for Ero1-Lα. The Cys^{94}-Cys^{99} cysteine pair of Ero1-Lα (corresponding to Cys^{100}-Cys^{105} in Ero1p) faces the active site in the *a'* domain of hPDI.

the Ero1-Lα-mediated oxidative folding. The C-terminal active site (in domain *a'*) is much more active than the N-terminal active site (in domain *a*) when Ero1-Lα is the source of oxidation. The difference of the two active sites is not thought to be due to their intrinsic catalytic properties, since they are reported to have a similar redox potential of −175 mV (27) and showed similar abilities to re-activate RNase A when GSSG is the source of oxidizing equivalents. If the two catalytic domains were exchanged positionally, the active site in domain *a* became more active than the one in domain *a'*. Pull-down and ITC assays confirmed that *b'xa'* is critical for binding with Ero1-Lα as well as for functional electron transfer. Thus, we attributed this asymmetry to the specific order of the two catalytic domains in the context of the full-length hPDI. In other words, the principal Ero1-Lα-binding site *b'xa'* on hPDI supplies the structural basis for the preference of Ero1-Lα to oxidize the active site next to the C-terminal of *bb'x* (Fig. 8).

Although a similar asymmetric effect was observed in terms of the oxidation rate of the two active sites in yeast PDI (yPDI) by Ero1p (28), it was claimed that the *b'* domain in yPDI is not required for recognition by Ero1p, in contrast to the necessary role of the *b'* domain of hPDI with Ero1-Lα. This claim is rather surprising, since the *b'* domain of hPDI has been characterized to contain the principal substrate binding site (5, 29), and a hydrophobic pocket in yPDI *b'* was also identified in the crystal structure (4). In hPDI the *b'* domain is sufficient for the binding of short peptides and essential for the binding of more complex substrates, while the *a* and *a'* domains also contribute to the binding of larger substrates (29). It was also reported that the minimum requirement for assembly of collagen prolyl 4-hydroxylase tetramer is fulfilled by domains *b'* and *a'* of hPDI, and the presence of the *a* and *b* domains greatly enhances assembly (30). Our recent study on ERp44, a PDI family member, has shown that a hydrophobic pocket in domain *b'* and a hydrophobic patch in domain *a* could be potential binding sites for client proteins, including Ero1-Lα (20). All the evidence above strongly support our finding that the *b'xa'* region is the minimal element for binding with Ero1-Lα, and all domains together fulfill the maximum binding. One consequence of this conclusion is that both Ero1-Lα and substrate proteins share a common binding site on PDI and hence that PDI must interact sequentially with these partners when transferring oxidizing equivalents from the oxidase to a reduced protein substrate (rather than interacting with both in a ternary complex of Ero1-Lα/PDI/reduced protein).

A basic question in the oxidative folding in the ER is the pathways or networks of electron flows. In prokaryotic periplasm, the oxidation (operated by the DsbA/DsbB system) and the reduction/isomerization (operated by the DsbC/DsbD system) pathways are kinetically separated (31). In eukaryotic ER, glutathione (GSH/GSSG) has long been considered to provide the principal redox buffer implicated in the formation of native protein-disulfide bonds (32). The ratio of GSH/GSSG in the secretory pathway is 1:1–3:1, far more oxidizing than the cytosolic ratio of 30:1–100:1 (33, 34) and similar to the optimum GSH/GSSG ratio of 5:1 for *in vitro* folding of disulfide bond-containing proteins (19). However, the discovery of Ero1 as the essential oxidase relaying oxidizing equivalents from molecular oxygen for the formation of protein disulfide bonds (9, 10) raised questions on the role of GSH/GSSG in oxidative folding in the ER. In this work, we clearly showed that the oxidative protein folding process can be facilitated by Ero1-Lα and hPDI, independent of any bulk redox buffer. However, these data cannot exclude the possibility that GSH/GSSG functions

as a redox buffer in the ER with GSSG providing oxidizing equivalents to PDI or directly to protein substrates in some circumstances, while GSH is responsible for the reduction of non-native disulfide bonds directly or indirectly in the ER (32), The absence of such a reducing function in the reconstituted Ero1-Lα/hPDI oxidative protein folding system may explain why this system is less active in reactivation of reduced RNase A than the simpler system of PDI plus GSH/GSSG (Fig. 4).

Another intriguing question is how is the redox homeostasis in the ER maintained under various conditions? Recently, a feedback mechanism was proposed to regulate the homeostasis in the ER through modulation of Ero1p activity by changing the redox state of the regulatory cysteine pairs (35). Our results from Ero1-Lα together with previous report on Ero1p (18, 22, 35) suggest that Ero1 can oxidize various vicinal dithiols such as DTT, Trx_{red}, and PDI but not monothiols (GSH) or multi-thiols (RNase A) where the thiols cannot form a stable vicinal disulfide. This property of Ero1 could be very important for maintaining the redox homeostasis in the ER by, for example: 1) effectively eliminating hyperreducing agents, such as DTT, thus protecting cells from reductive stress; 2) passing oxidizing equivalents to protein substrates via PDI, an ER oxidoreductase with proofreading (isomerase) activity, rather than directly introducing non-native disulfides into substrates; 3) avoiding the futile consumption of reducing equivalents in GSH, which can itself reduce efficiently non-native disulfide bonds as well as reactive oxygen species generated by Ero1 activity.

Acknowledgments—We thank Prof. R. Sitia, Università Vita-Salute San Raffaele, Italy, for the generous gift of the Ero1-Lα cDNA. We gratefully acknowledge Prof. J. D. Zhao and Dr. X. W. Liu, Peking University, for kind help with the oxygen consumption assay.

REFERENCES

1. Sevier, C. S., and Kaiser, C. A. (2006) *Antioxid. Redox Signal.* **8,** 797–811
2. Freedman, R. B., Klappa, P., and Ruddock, L. W. (2002) *EMBO Rep.* **3,** 136–140
3. Ellgaard, L., and Ruddock, L. W. (2005) *EMBO Rep.* **6,** 28–32
4. Tian, G., Xiang, S., Noiva, R., Lennarz, W. J., and Schindelin, H. (2006) *Cell* **124,** 61–73
5. Pirneskoski, A., Klappa, P., Lobell, M., Williamson, R. A., Byrne, L., Alanen, H. I., Salo, K. E. H., Kivirikko, K. I., Freedman, R. B., and Ruddock, L. W. (2004) *J. Biol. Chem.* **279,** 10374–10381
6. Yao, Y., Zhou, Y. C., and Wang, C. C. (1997) *EMBO J.* **16,** 651–658
7. Tsai, B., Rodighiero, C., Lencer, W. I., and Rapoport, T. A. (2001) *Cell* **104,** 937–948
8. Uehara, T., Nakamura, T., Yao, D. D., Shi, Z. Q., Gu, Z. Z., Ma, Y. L., Masliah, E., Nomura, Y., and Lipton, S. A. (2006) *Nature* **441,** 513–517
9. Frand, A. R., and Kaiser, C. A. (1998) *Mol. Cell* **1,** 161–170
10. Pollard, M. G., Travers, K. J., and Weissman, J. S. (1998) *Mol. Cell* **1,** 171–182
11. Sevier, C. S., and Kaiser, C. A. (2008) *Biochim. Biophys. Acta* **1783,** 549–556
12. Cabibbo, A., Pagani, M., Fabbri, M., Rocchi, M., Farmery, M. R., Bulleid, N. J., and Sitia, R. (2000) *J. Biol. Chem.* **275,** 4827–4833
13. Pagani, M., Fabbri, M., Benedetti, C., Fassio, A., Pilati, S., Bulleid, N. J., Cabibbo, A., and Sitia, R. (2000) *J. Biol. Chem.* **275,** 23685–23692
14. Mezghrani, A., Fassio, A., Benham, A., Simmen, T., Braakman, I., and Sitia, R. (2001) *EMBO J.* **20,** 6288–6296
15. Bertoli, G., Simmen, T., Anelli, T., Molteni, S. N., Fesce, R., and Sitia, R. (2004) *J. Biol. Chem.* **279,** 30047–30052
16. Li, S. J., Hong, X. G., Shi, Y. Y., Li, H., and Wang, C. C. (2006) *J. Biol. Chem.* **281,** 6581–6588
17. Bradford, M. M. (1976) *Anal. Biochem.* **72,** 248–254
18. Gross, E., Sevier, C. S., Heldman, N., Vitu, E., Bentzur, M., Kaiser, C. A., Thorpe, C., and Fass, D. (2006) *Proc. Natl. Acad. Sci. U. S. A.* **103,** 299–304
19. Lyles, M. M., and Gilbert, H. F. (1991) *Biochemistry* **30,** 613–619
20. Wang, L. K., Wang, L., Vavassori, S., Li, S. J., Ke, H. M., Anelli, T., Degano, M., Ronzoni, R., Sitia, R., Sun, F., and Wang, C. C. (2008) *EMBO Rep.* **9,** 642–647
21. Tu, B. P., and Weissman, J. S. (2002) *Mol. Cell* **10,** 983–994
22. Tu, B. P., Ho-Schleyer, S. C., Travers, K. J., and Weissman, J. S. (2000) *Science* **290,** 1571–1574
23. Wilkinson, B., Xiao, R., and Gilbert, H. F. (2005) *J. Biol. Chem.* **280,** 11483–11487
24. Kozlov, G., Maattanen, P., Schrag, J. D., Pollock, S., Cygler, M., Nagar, B., Thomas, D. Y., and Gehring, K. (2006) *Structure* **14,** 1331–1339
25. Gruber, C. W., Cemazar, M., Heras, B., Martin, J. L., and Craik, D. J. (2006) *Trends. Biochem. Sci.* **31,** 455–464
26. Frickel, E. M., Riek, R., Jelesarov, I., Helenius, A., Wuthrich, K., and Ellgaard, L. (2002) *Proc. Natl. Acad. Sci. U. S. A.* **99,** 1954–1959
27. Lundstrom, J., and Holmgren, A. (1993) *Biochemistry* **32,** 6649–6655
28. Kulp, M. S., Frickel, E. M., Ellgaard, L., and Weissman, J. S. (2006) *J. Biol. Chem.* **281,** 876–884
29. Klappa, P., Ruddock, L. W., Darby, N. J., and Freedman, R. B. (1998) *EMBO J.* **17,** 927–935
30. Pirneskoski, A., Ruddock, L. W., Klappa, P., Freedman, R. B., Kivirikko, K. I., and Koivunen, P. (2001) *J. Biol. Chem.* **276,** 11287–11293
31. Nakamoto, H., and Bardwell, J. C. A. (2004) *Biochim. Biophys. Acta* **1694,** 111–119
32. Chakravarthi, S., Jessop, C. E., and Bulleid, N. J. (2006) *EMBO Rep.* **7,** 271–275
33. Hwang, C., Sinskey, A. J., and Lodish, H. F. (1992) *Science* **257,** 1496–1502
34. Bass, R., Ruddock, L. W., Klappa, P., and Freedman, R. B. (2004) *J. Biol. Chem.* **279,** 5257–5262
35. Sevier, C. S., Qu, H. J., Heldman, N., Gross, E., Fass, D., and Kaiser, C. A. (2007) *Cell* **129,** 333–344